

IMPLICATIONS AND APPLICATIONS OF KINEMATIC GALAXY SCALING RELATIONS

DENNIS ZARITSKY

Steward Observatory, University of Arizona, 933 North Cherry Avenue, Tucson, AZ 85721
Invited Spotlight Article for IRSN Astronomy and Astrophysics

ABSTRACT

Galaxy scaling relations, which describe a connection between ostensibly unrelated physical characteristics of galaxies, testify to an underlying order in galaxy formation that requires understanding. I review the development of a scaling relation that 1) unites the well-known Fundamental Plane (FP) relation of giant elliptical galaxies and Tully-Fisher (TF) relation of disk galaxies, 2) fits low mass spheroidal galaxies, including the ultra-faint satellites of our Galaxy, 3) explains the apparent shift of lenticular (S0) galaxies relative to both FP or TF, 3) describes all stellar dynamical systems, including systems with no dark matter (stellar clusters), 4) associates explicitly the numerical coefficients that account for the apparent “tilt” of the FP away from the direct expectation drawn from the virial theorem with systematic variations in the total mass-to-light ratio of galaxies within the half-light radius, 5) connects with independent results that demonstrate the robustness of mass estimators when applied at the half-light radius, and 6) results in smaller scatter for disk galaxies than the TF relation. The relation develops naturally from the virial theorem, but implies the existence of additional galaxy formation physics that must now be a focus of galaxy formation studies. More pragmatically, the relation provides a lynchpin that can be used to measure distances and galaxy masses. I review two applications: 1) the cross-calibration of distance measurement methods, and 2) the determination of mass-to-light ratios of simple stellar populations as a function of age, and implications of the latter for the stellar initial mass function.

1. INTRODUCTION

To develop an understanding of any set of objects, we first classify them in the expectation that this will help us uncover the rules that describe the set. For stars, this systematic approach led to stellar classification, eventually to the Hertzsprung-Russell diagram, and finally to theories of stellar structure and nuclear burning that comprise one of astronomy’s fundamental successes of the previous century. For galaxies, this approach has been less successful in uncovering simple intuitive guiding principles. In part, this failure was due to the absence of a comprehensive description of galaxy structure akin to that available for stars. Theories of galaxy formation, currently represented mostly by numerical simulations (for example see Springel et al. 2005), are left to describe a loosely tied set of observables that include galaxy luminosity functions, clustering properties, color distributions, and star formation rates for ensembles of systems, rather than the specific characteristics of any individual galaxy. As such, even if these models successfully reproduce the existing ensemble observations, our understanding of galaxies would be quite different in nature than our understanding of stars.

What does this long-running failure to identify simple rules of galactic structure signify? Perhaps it reflects a greater underlying complexity to galaxies than to stars. Perhaps the formation and evolution of galaxies is so strongly sensitive to different variables that each galaxy is an entirely distinct entity and we will never find a simple description of galaxy structure that is both broadly applicable and sufficiently precise for individual galaxies. Seen in this light, it becomes clear that the search for the unifying principles of galactic structure is

in essence an attempt to determine the degree to which simple, intuitive guiding principles for galaxy formation can accurately describe real galaxies at a non-trivial level of detail. At its core, this is an argument between the potential value of an analytic description of galaxy formation vs. the need for numerical simulations.

In this article, I describe recent work that has demonstrated that there is indeed an underlying simple order to stellar systems of all types and masses beyond that which we can currently explain. The observed low scatter about this empirical relationship, which ties together the basic measurable properties of galaxies, attests to the presence of underlying rules. Perhaps the low scatter arises from a galaxy formation version of the central limit theorem or, perhaps, it points to a more intuitively meaningful connection between the way stars form and are packed within dark matter potentials. I frame the discussion of the relationship in terms of assumptions and refinements to the virial theorem as applied to galaxies to clarify the additional constraints and information provided by the empirical findings. I will show how this new scaling relation helps address a number of open questions, including some regarding the nature of S0 and low luminosity galaxies, while at the same time being applicable to all of the galaxies that were well described by the Fundamental Plane (FP) and Tully-Fisher (TF) relations. After describing this scaling relationship, which is referred to as the Fundamental Manifold (FM), in reference to its antecedent the FP, I proceed to describe ways in which it can be exploited to measure other quantities of core astrophysical interest, distances and galaxy masses.

2. A LOGICAL PATH TO GALAXY SCALING RELATIONS

Over time, a disjoint set of rules regarding galaxy structure, generally referred to as scaling relations, have been identified (for some examples see Faber & Jackson 1976; Kormendy 1985; Burstein et al. 1997; Khosroshahi et al. 2000; Graham 2002). The two such relations that are in most common use, and include measurements of the internal kinematics of galaxies, are the Tully-Fisher relationship (TF; Tully & Fisher 1977) and the Fundamental Plane (FP; Djorgovski & Davis 1987; Dressler et al. 1987). Quantitatively, however, these are somewhat arcane parameterizations, with non-integer coefficients that are derived empirically and depend on observational details such as filter passbands (for example see Pizagno et al. 2007). Qualitatively, these differ from one another in that they apply to restricted, non-overlapping sets of galaxy types and are functions of different measured quantities. These relations are therefore at best partial answers in our quest for a comprehensive description of galactic structure. As usual, with the benefit of hindsight, one can rework a clearer narrative. We now trace a straightforward, contiguous path to the FP and TF that will explain certain features of those relationships, and to the unification of those relationships into one proposed as being applicable to all stellar systems (Zaritsky et al. 2006a, 2008).

2.1. Starting From the Virial Theorem

It is a common misconception that the scaling relations are simply rephrased versions of the virial theorem. Although their origin lies with that theorem, their existence implies additional, non-trivial, physical constraints on the nature of galaxy formation. This assertion is clarified by expressing the virial theorem in a form reminiscent of the FP:

$$\log r_0 = 2 \log V_0 - \log I_0 - \log \Upsilon_0 + \log A_0 - \log B_0 - C_0, \quad (1)$$

where the subscript 0 indicates quantities measured at a selected radius, r_0 : V_0 is a measure of the internal motions within that radius (typically either the circular velocity, velocity dispersion, or some combination), I_0 is the surface brightness within r_0 , Υ_0 is the mass-to-light ratio of the matter within r_0 , A_0 and B_0 are coefficients arising from the integration of the kinetic and potential energy terms in the virial theorem (setting, for example, $\int_0^\infty v^2 r^2 dr \equiv AV^2$), and finally C_0 is an integration constant. In principle, r_0 should be selected to encompass the entire system because the virial theorem applies to the system as a whole. However, in practice, because galaxies have no well-defined edges and the low surface brightnesses of their outskirts make measuring these quantities difficult, r_0 is selected to be a compromise radius, such as that which encompasses half the light of the system, r_h . This is the first step away from the formal (physically correct) application of the virial theorem.

Additional assumptions and simplifications are necessary to apply Eq. 1 to real systems. Because A , B , C , and Υ can vary from system to system, and also for different enclosed radii within the same system, there is no *a priori* assurance that Equation 1 defines a simple, limited distribution of galaxies within the (r_0, I_0, V_0) space, aka a *scaling relation*. In other words, solutions

of Equation 1 exist for any combination of (r_0, I_0, V_0) if Υ_0 , A_0 , B_0 , and C_0 are unconstrained, and yet galaxies do not populate the entire (r_0, I_0, V_0) -space. The more confined the distribution of galaxies within this space, the more restrictive the constraints on the models. The value of a scaling relation is that it quantifies the degree to which nature is limiting combinations of these parameters, and, by implication, underlying additional physics that we have yet to appreciate that lies beyond the virial theorem. If galaxies are found only in limited combinations of r_0 , I_0 , and V_0 , then it must also be true that only certain combinations of A_0 , B_0 , C_0 and Υ_0 are allowed. Why?

2.2. A Key Simplification

I now take a slight detour in our quest for a comprehensive scaling relation by considering an important result regarding the measurement of galaxy masses. The virial theorem, and hence Equation 1 in a slightly different guise, is also the primary pathway to galaxy mass determinations because it can be used to measure Υ . The difficulty that underlies all such discussions (for examples see, Page 1952; Bahcall & Tremaine 1981; Heisler et al. 1985; Erickson et al. 1987; Little & Tremaine 1987; Zaritsky & White 1994) is evident from our expression of the virial theorem in Equation 1, namely the unknown numerical values of A , B , and C , hereafter referred to as the virial coefficients. For simple geometries these coefficients can be evaluated analytically, for example the gravitational potential energy for a uniform density sphere is $3GM^2/5R$, leading to $B = 3G/5$ in this particular example. However, in reality these coefficients are particularly troublesome because we have no way to calculate them without having a full knowledge of the gravitational potential and the tracer particle distribution function and no guarantee that whatever values we adopt remain at least roughly constant from system to system.

In the face of such ignorance, one usually adopts the simplest possibility — that these values are the same from galaxy to galaxy — and then proceeds to use simple modeling or back-of-the-envelope arguments to obtain numerical values that are inserted into the analogs of Eq. 1 (often referred to as mass estimators: Bahcall & Tremaine 1981; Zaritsky & White 1994). In certain cases, additional data, such as measurements of the higher order moments of the line of sight velocity distribution, constrain the orbits of the tracer particles (Smith & Gray 1976; Dejonghe 1987; Merrifield & Kent 1990), providing independent information on the virial coefficients. These approaches typically center on the application of the Jeans equation (for example see Merrifield & Kent 1990) or Schwarzschild modeling (for a few examples see Vandervoort 1984; Statler 1987; Cretton et al. 1999) to help in the interpretation of the data, but both require data that is far superior than what is typically available. Nevertheless, such studies provide critical tests for any less sophisticated method, assuming that such methods are not inherently doomed by system to system variations in the values of the virial coefficients. The key prerequisite to the use of mass estimators is establishing that variations in the virial coefficients are not the dominant source of uncertainty.

Walker et al. (2009) and Wolf et al. (2010) demon-

strated, using a range of dynamical models for spheroidal galaxies, that the enclosed mass *at the half light radius*, M_h , as estimated from easily measured observables (size, luminosity, and velocity dispersion), is robust to the unknown details of the internal kinematics and structure of the stellar system (robust to $\sim 10\%$ or 0.05 dex, Wolf et al. 2010). Those studies were motivated by the desire to measure accurate and precise masses for low mass stellar systems as tests of hierarchical structure formation models and dark matter halo profiles¹. However, in the language of Equation 1, those studies show that the virial coefficients are materially identical from system to system — *if one applies the equation at the half-light radius, r_h* . Correspondingly, they also show that if one attempts to use analogs of Eq. 1 for quantities measured at radii other than r_h one will realize more scatter in the mass estimates. This work demonstrates that the success of the FP, and the extended scaling relation we discuss here, lies in large part to a fortuitous choice of r_h as the scaling relation’s fiducial radius. The value of the Walker et al. (2009) and Wolf et al. (2010) work, in the context of the current discussion, is that it codified what had generally been assumed without much supporting evidence and also highlighted when and how the assumption breaks down.

Using the results of that work, I calculate a numerical value for the combined quantity $\log A_h - \log B_h - C_h$ in Equation 1. Walker et al. (2009) find that $M_h = 580 r_h \sigma_v^2$, where the mass is in solar masses, r_h is in pc, and σ_v is the line of sight velocity dispersion² in km s^{-1} . Rewriting this expression in a form similar to Eq. 1 by defining $I_h \equiv L_h / \pi r_h^2$ and converting units, results in

$$\log r_h = 2 \log \sigma_v - \log I_h - \log \Upsilon_h - 0.73 \quad (2)$$

comparing Eqns. 1 and 2 highlights the obvious similarity and leads us to associate σ_v with V for spheroidal galaxies and conclude that $\log A_h - \log B_h - C_h = -0.73$. The derived value of the combined virial coefficients in Equation 2 can be tested by comparing mass estimates within r_h obtained using the more robust methods (Jeans or Schwarzschild modeling and/or gravitational lensing model (Bolton et al. 2008)) to those obtained by applying Equation 2 to get Υ_h and then multiplying by the luminosity L_h . Following that approach, Zaritsky et al. (2008) independently (prior to the Walker et al. (2009) study) found a combined value of the virial coefficients of -0.75 , in what turned out to be excellent agreement with Equation 2. Confirmation that the combined virial coefficients are roughly the same from system to system comes from the low scatter about Equation 2 of real systems with independently determined values of Υ_h (see Zaritsky et al. 2008).

¹ Wolf et al. (2010) argue further that the true half-mass radius, rather than the projected half-mass radius works best, while Walker et al. (2009) present an analysis in projected space. The two results are consistent and we opt to use the Walker et al. (2009) result which involves projecting models rather than deprojecting the observations.

² We explicitly add the subscript v to σ to specify that it represents a *velocity* dispersion. However, in cases where we want to highlight some other aspect of σ , for example that it is measured within the half-light radius, r_h , we will drop the subscript v and replace it with the subscript h , as in σ_h . Nevertheless, σ always refers to the line-of-sight velocity dispersion if it carries any subscript.

Once the system-to-system stability of the virial coefficients is confirmed and accepted, the last remaining unknown in Eq. 2 is Υ_h . Observationally, the scatter about the Fundamental Manifold (FM) is limited to ~ 0.1 dex, and is even smaller for subsamples of galaxies drawn from the individual studies that comprise the heterogeneous dataset in that work (Zaritsky et al. 2008). However, even if the scatter were zero, it would still be the case mathematically, that any combination of (r_h, σ_h, I_h) would be allowed by Equation 2 if Υ_h is unconstrained³. The existence of a scaling relation, where galaxies populate a very limited region of (r_h, σ_h, I_h) -space also implies that Υ_h is constrained.

For dark matter free systems, the structure is now entirely defined if one evaluates Υ_h using simple stellar population models. Because most of the stellar clusters for which the set of (r_h, σ_h, I_h) exist are old (> 10 Gyr), they should have nearly the same value of Υ_h (even if they are all of the same age, variations in Υ_h will exist due to chemical abundance variations and dynamical evolution). With Υ_h set to a constant, Equation 2 describes a plane in the $\log r_h - \log \sigma_h - \log I_h$ -space. Indeed, Milky Way globular clusters not only fall onto a plane, they fall onto a line (Pasquato & Bertin 2008; Zaritsky et al. 2011), which suggests even further constraints on their structure, specifically an underlying relationship between two of the three measured parameters that removes an additional degree of freedom⁴.

2.3. Onward to the Fundamental Plane

Giant elliptical galaxies empirically obey the FP, which has the form

$$\log r_h = \beta \log \sigma_v - \gamma \log I_h + \delta, \quad (3)$$

where β , γ , and δ are numerical coefficients. This relationship lacks the troublesome Υ_h that is included in Eq. 2. Within the framework of Eq. 2, the validity of the FP therefore requires that $\Upsilon_h \propto \sigma_v^{2-\beta} I_h^{1+\gamma}$, for those galaxies that occupy the FP. One particular published fit to the FP, $r_h \propto \sigma_v^{1.2 \pm 0.07} I_h^{-0.82 \pm 0.02}$ from Cappellari et al. (2006), therefore implies that $2 - \beta = 0.8 \pm 0.07$ and $1 + \gamma = -0.18 \pm 0.02$, or expressed in another form, that $\Upsilon_h \propto \sigma_v^{0.8} I_h^{-0.18}$ for the giant elliptical galaxies that satisfy the FP. Although alternative fits of the FP exist using different samples of ellipticals that are often observed in different filter pass bands (for examples see Jørgensen et al. 1996; Bernardi et al. 2003), they differ in detail rather than in spirit. All of these relations implicitly require that the mass-to-light ratio have power-law dependence on σ_v and I_h .

The relationship between the total mass-to-light ratio and the structural properties of galaxies must arise from physics that dictates how luminous baryons settle into dark matter potential wells. As such, it is critical to understand if this relationship holds for more

³ The only obvious physical constraint on Υ_h is the lower limit defined by the mass-to-light ratio of a purely stellar population.

⁴ Qualitatively such constraints are not difficult to imagine. For example, a cluster with extremely low surface density might not have been able to form simply because the cloud from which it would have formed would have been tidally disrupted. Nevertheless, the quantitative constraint on formation models provided by Eq. 2 could be quite challenging and informative

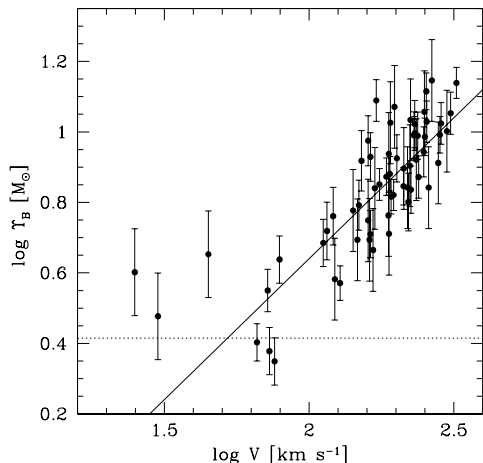


Figure 1. Υ in the B-band for local galaxies from van der Marel & van Dokkum (2007) using a Jeans equation analysis. Here we take $V = \sigma_v$ and have plotted all 62 of their systems. The dotted line represents an estimate of Υ for a purely stellar population. The solid line represents the expectation based on the σ_v dependence inferred from the Cappellari et al. (2006) FP.

than giant elliptical galaxies. Using direct measurements of Υ_h from Jeans modeling (Figure 1; data from van der Marel & van Dokkum 2007) we see both that the power law relationship between Υ_h and σ_v holds for giant ellipticals consistent with the slope inferred above, 0.8, as it must due to their obeying the FP, and that it breaks down for low σ_v ellipticals. It is not surprising that the power-law description breaks down for low σ_v because extrapolating the power law leads to unphysical values of Υ_h that are smaller than those of a dark-matter-free stellar population (the dotted line in the Figure). On the basis of these data, the FP is manifestly only valid for galaxies above a threshold $\sigma_v \sim 100 \text{ km sec}^{-1}$. The full relationship between Υ_h and (σ_v, I_h) must therefore be more complex than a power-law. In addition to the flattening at low σ_v seen in Figure 1, there is also evidence for a turnover, or deviations from the FP, at large values of σ_v (Zaritsky et al. 2008; Bernardi et al. 2011).

The FP is not an all-inclusive scaling relation, even considering only spheroidal galaxies. The relationship between Υ_h and σ_v must be of higher complexity than presumed in the FP (Zaritsky et al. 2008; Tollerud et al. 2011). The FP applies only where a power law description is an acceptable approximation to this more complicated relationship. Although the simple power-law description of Υ_h fails, this failure is not a conceptual problem because there was never any physical motivation for such straightforward behavior. However, Υ_h can be described as a function of σ_v even when σ_v is $< 100 \text{ km sec}^{-1}$ if one is will to consider a more complex analytic description for the structure of galaxies.

2.4. Incrementally Adding Rotation

Even ignoring the galaxies with low σ_v in Fig 1, the FP is only valid for galaxies whose stellar distribution is dynamically supported by stellar random motions. We must therefore search for a description that is more broadly applicable than the FP. In cer-

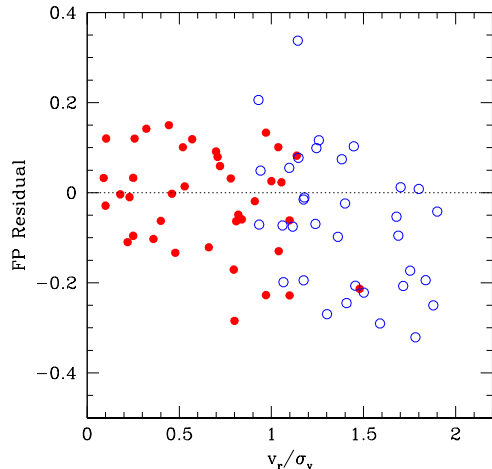


Figure 2. Deviation from the FP as a function of v_r/σ_v for two galaxy samples, ellipticals from van der Marel & van Dokkum (2007) (filled red) and S0's from Bedregal et al. (2006) (open blue). As v_r/σ_v increases the deviations become systematic and negative, indicating some dependence on v_r is needed in the scaling relation. The interpretation of this trend is that the FP is not accounting for the dynamical support provided by rotation and that this omission causes larger deviations as the rotational support becomes more important.

tain early-type galaxies, lenticulars in particular, but also lower luminosity spheroidals (Davies et al 1983; Bender 1990), rotation provides an important additional source of dynamical support. This support is evident in the classic diagram comparing the ratio of the rotational velocity, v_r , to the velocity dispersion, v_r/σ_v , vs. ellipticity (Davies et al 1983), but also becomes evident when plotting the deviation from the FP (using the parameterization $r_h \propto \sigma_v^{1.2 \pm 0.07} I_h^{-0.82 \pm 0.02}$ from Cappellari et al. (2006)) vs. v_r/σ_v using data for ellipticals (van der Marel & van Dokkum 2007) and S0's (Bedregal et al. 2006) in Figure 2.

As galaxies become more rotationally supported, the use of only σ_v to measure their dynamical support leads to a systematic deviation from the FP. Therefore, a natural extension of the FP invokes a combination of σ_v and v_r , referred to here as V , to describe this support. The commonly suggested combination is expressed as $V = \sqrt{v_r^2/\alpha + \sigma_v^2}$, where α is a parameter that is determined by the internal structure of the system. Unfortunately, the existing data are insufficient to discriminate between choices of α suggested previously (Burstein et al. 1997; Weiner et al. 2006; Kassin et al. 2007; Zaritsky et al. 2008). A standard choice is $\alpha = 2$, although $\alpha = 3$ is also acceptable (Weiner et al. 2006) and Zaritsky et al. (2008) fit the data to argue for $\alpha = 2.68$. The allowed range in values of α is related to the unknown nature of the gravitational potential and the tracer particle distribution function. Within an isothermal potential, if the orbits are isotropic, then $\alpha = 2$, while for other potentials and orbital anisotropies the value of $\alpha \neq 2$. Here, we will simply adopt $\alpha = 2$. Although the value of α is critical for certain applications, such as determining whether subtle variations in the value of Υ_h exists between ellipticals and S0's, it is not

so for the discussion here. In general, for pressure supported systems V reduces to σ_v , which is what we used in our discussion of giant ellipticals, and for purely rotationally supported galaxies V reduces to $v_r/\sqrt{\alpha}$, which is what we will use for late type galaxies and then only affects the normalization of the late-types relative to the early types on the FM. We now proceed to discuss the inclusion of late-type galaxies in this context⁵.

It is evident from Figure 2 that some of the scatter in the FP, even among ellipticals, comes from neglecting rotational support and that studies that use the FP to search for stellar population differences among early-types, for example those searching for differences among galaxies in different environments, could face systematic errors if the degree of rotational support differs in systematic ways. This issues could even trickle down to the interpretation of studies that do not use the FP, but use σ_v as an indication of mass (Zhu et al. 2010).

2.5. Onward to and Beyond the Tully-Fisher Relationship

Unlike the FP, the TF does not involve a radial scale and it has resisted improvement (i.e. a reduction in scatter) via the addition of other structural parameters (Aaronson & Mould 1983). The lack of scale dependence is a bit puzzling in that one would expect a galaxy that is physically twice as large as another, but with the same rotation velocity, to have twice as much mass and hence twice the luminosity. As such, the existence of the TF implies that the larger galaxy must have a commensurate lower surface brightness (so that it does not have a higher total luminosity) — and that this tradeoff must be nearly balanced to avoid the expected scale dependence. Some hints of a radial dependence are appearing with larger datasets and better data. While these studies suggest that this balance is not exact (Courteau et al. 2007; Saintonge & Spekkens 2011), we again see that the existence of scaling relations requires that the process of galaxy formation results in systematic packing of the luminous baryons. For disks, analytic formation models have long advocated a connection between the specific angular momentum of the baryons and surface density or disk size (Fall & Efstathiou 1980; Dalcanton et al. 1997), which goes part of the way to explaining this balance. Furthermore, systematic behavior between rotation curves and dark matter halos has been identified (Salucci et al. 2007), which demonstrates the existence of connections between the formation of the entire galaxy and the properties of the inner, observable component.

Because we seek a universal scaling relation, I avoid the TF for now and assert that Eq. 2, inclusive of the combined kinematic support from v_r and σ_v , should apply to late type galaxies. I therefore rewrite the FP as an expression for the luminosity, L , for comparison to TF, again using the Cappellari et al. (2006) parameterization of the FP,

$$L = 1.2 \log V + 0.18 \log I_h + r_h + \text{Constant} \quad (4)$$

⁵ In principle, one can determine the value of α by requiring agreement between early and late type galaxies for a single value of the constant in Eq. 2. However, in practice because of the dichotomy between FP and TF studies, the samples of early and late type galaxies have been observed and analyzed differently and small differences in photometric systems or analysis technique are sufficient to explain the offsets found.

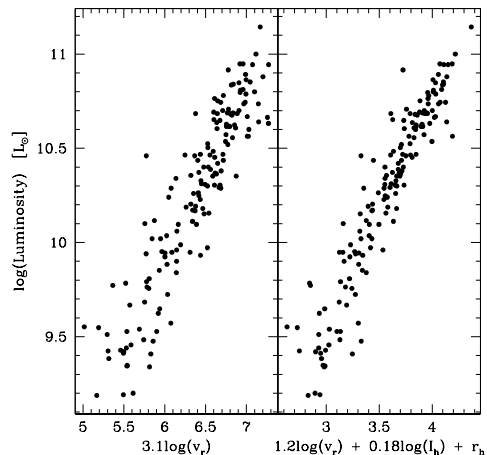


Figure 3. Predictions of galaxy luminosity from TF and our rewritten FP for disk galaxies. We compare the predicted luminosities (x-axis) to measured luminosities using the galaxies Hubble distance (y-axis) for galaxies from the Pizagno et al. (2007) study using their best-fit TF relationship (left panel) to and that using our re-expression of the Cappellari et al. (2006) FP relation and the use of the V parameter (right panel). The scatter is evidently smaller in the right panel (0.75 in the left one, 0.47 in the right), showing that including a radial scale, as is done in the FM, adds significant information.

In Figure 3, I compare the predictions of L from the TF (i.e. using the circular velocity and the best fit TF relation presented by Pizagno et al. 2007) and from the rewritten FP (Equation 4) with the luminosities inferred using distances calculated from their recessional velocities for disk galaxies with $V > 100 \text{ km sec}^{-1}$ (because the FP applies only to such galaxies). I use the Pizagno et al. (2007) study because it is one of the few TF samples that includes measurements of r_h . The scatter is visibly lower in the re-written FP relation than in the TF relation (0.47 vs. 0.75), demonstrating that the FM parameterization is at least as good as the best-fit TF. Previous studies that searched for a scale dependence may have had a difficult time finding one because they either used different radii than r_h , such as the disk scale length or an isophotal radius, or faced additional noise from not using the rotational velocity at or near r_h . Although for disk galaxies, with their mostly circular orbits, one can argue that $M \propto rv_r^2$ should be a fairly good approximation regardless of which of the standard fiducial radii (disk scale, isophotal, half light) is chosen (see Yegorova & Salucci 2007, for empirical support for this claim), the only one of these radii that has a direct connection to the total luminosity is the half light radius.

To see how the TF is a subset of the relationships allowed by Eq. 2, I begin with the TF relation

$$L = Av_r^\delta, \quad (5)$$

where A and δ are constants, rewrite the expression using the definition of I_h , and rearrange it to be in the form of Eq. 1,

$$\log r_h = \delta \log v_r - \log I_h + \text{Constant}. \quad (6)$$

Again there is a strong similarity to Eq. 2 and the validity of both equations for giant spiral galaxies sug-

gests that $V = v_r$ and that $\Upsilon_h \propto v_r^{2-\delta}$ for these spirals. Because empirically $\delta \sim 3 - 4$ (Pizagno et al. 2007; Courteau et al. 2007), Υ_h decreases as v_r increases. Therefore, it is wrong to accept that the TF applies in general because, like the FP, it too faces a fundamental conceptual flaw if extended beyond the class of galaxy from which it was derived. The FP predicts unphysical values of Υ_h for low σ_v systems. The TF predicts unphysical values of Υ_h for high v_r galaxies. Therefore, just as in the case of the FP, some curvature in the relation is necessary for disk galaxies. Suggestions of nonlinearity in the TF relation have existed for over 20 years (Mould et al. 1989; Persic & Salucci 1991). Neither the FP nor TF hold across all galaxy masses, and a more complex relation is needed between Υ_h and V .

2.6. Closure on a Universal Galaxy Kinematic Scaling Relation

Returning to Equation 1, we see that the three ingredients involved in arriving at a universal galaxy scaling relation are 1) the virial theorem, 2) the robustness of mass estimates at the half light radius, which affirms that the virial coefficients are relatively independent of the detailed structure and kinematics of each galaxy, and 3) the relationship between Υ_h and the directly measurable structure parameters (r_h, V_h, I_h). The first is a natural expectation for collapsed systems, particularly since $r_h \ll r_{virial}$. The second has been demonstrated by Walker et al. (2009) and Wolf et al. (2010) but has been evident in the low empirical scatter of the scaling relations for decades. The last remains perhaps the most mysterious because it involves a connection between the efficiency of star formation and the packing of those stars within dark matter halos of galaxies. Understanding this behavior is particularly challenging given that the values of Υ_h for galaxies vary between values of ~ 1 and ~ 1000 . This behavior lies at the core of understanding galaxy formation.

The classic scaling relations, FP and TF, implicitly adopt a power-law scaling between Υ_h and the observables. This description fails as we proceed to either low (Figure 1) or high σ_v galaxies. The power-law assumption must be abandoned. A more complicated manifold relates the observables to Υ_h and was named the Fundamental Manifold (Zaritsky et al. 2006a) in reference to its antecedent the FP. In the interest of completeness, I present one specific parameterization of that surface from Zaritsky et al. (2011)

$$\Upsilon_h = 1.49 - 0.32 \log V_h - 0.83 \log I_h + 0.24 \log^2 V_h + 0.12 \log^2 I_h - 0.02 \log V_h \log I_h. \quad (7)$$

However, because there is yet no set of homogeneous data that includes internal kinematics and spans all galaxy types and luminosities, the derivation of this surface remains preliminary and varies quantitatively depending on what sample is used. Additionally, there is no physical motivation for why the surface has any particular functional form. As such, larger samples that cover the full parameter space are critically needed. Should subsequent investigations define a completely different functional form for Υ_h , that finding would not invalidate any of the discussion presented so far other than Equation 7.

Similar curvature is seen in the behavior of Υ in

efforts to match the halo and stellar mass functions (van den Bosch et al. 2003; Yang et al. 2005) and lensing mass measurements and luminosities (Hoekstra et al. 2005; Madelbaum et al. 2006). Because the relationship is currently only empirical, the finding that all stellar systems can be modeled with a simple, smooth functional form is perhaps surprising — but it hints at rules governing galaxy formation that are currently not fully understood.

2.7. What Comes Next?

On the observational front, the refinement of the FM requires a homogeneous dataset that includes all galaxy types and luminosities and which is volume representative (not necessarily complete). Such data would enable 1) a determination of α , 2) tests of whether the scatter increases for certain classes of galaxies, which would address whether the virial coefficients are sufficiently constant across galaxy types, and 3) a determination of how the surface relating Υ_h to (V_h, I_h) is populated to identify additional constraints on galactic structure. Care should be taken to minimize sources of photometric scatter by choosing passbands that minimize variations arising from stellar population variations and extinction. The sample should consist of galaxies with independent distance estimators so that distance uncertainties contribute minimally to r_h . Currently, the distances are calculated using the recession velocities and an adopted value of the Hubble constant. 2-D kinematics would help address issues related to inclination corrections for rotation speeds and help in the measurement of σ_v and v_r in systems where both contribute noticeably to the dynamical support. The sample might also include more systems where Υ_h can be estimated in an independent manner, for example through the use of gravitational lensing. Finally, and particularly important for questions related to the nature of the luminous baryon distribution, it is necessary to have independent estimates the stellar mass-to-light ratio, Υ_* . One such approach at measuring Υ_* is to use infrared luminosities and colors (Meidt et al. 2012; Eskew et al. 2012), although these estimates depend on stellar population models, that have their own set of uncertainties. Should these uncertainties be sorted out in subsequent work, we would be able to use the FM and these estimates to uncover the dark matter fractions for all galaxies within r_h in a way now done only with more sophisticated modeling on smaller samples of galaxies (Cappellari et al. 2012).

3. DISCUSSION

3.1. The Bifurcation of Stellar Systems

The function that describes the relation between Υ_h and (V_h, I_h) is roughly parabolic along the V_h axis and power-law like along the I_h axis (Equation 7). The general shape places constraints on how baryons settle and become stars within dark matter potentials. However, an important aspect that I have mostly ignored so far is how this surface is populated. In particular, there is a bifurcation in the population at low V_h where two branches develop, one heading upward to large values of Υ_h , populated by the Local Group dwarf spheroidals (Zaritsky et al. 2006a; Tollerud et al. 2011; Salucci et al. 2012) and ultrafaint

galaxies (Zaritsky et al. 2011; Willman & Strader 2012), and another heading downward to low values of Υ_h , populated by ultracompact dwarf galaxies and star clusters (Mieske et al. 2008; Zaritsky et al. 2011). The question is whether this bifurcation points to a problem with the scaling relation (Forbes et al. 2008) or whether it is pointing to a fundamental difference between systems with and without dark matter halos (Zaritsky et al. 2011).

The bifurcation may lie at the heart of a physical distinction between galaxies and star clusters (Willman & Strader 2012) and the FM may be a way to help explore that division. In particular, it would be of interest to determine whether there are objects that lie between these two branches, or whether the branches are absolute (Misgeld & Hilker 2011). Unfortunately, strong selection effects come into play. At the extremely low surface brightnesses of the ultrafaint galaxies, these systems require star counts to detect and are therefore not within reach if they lie outside the Local Group. It may be possible, with the next generation of sky surveys, to detect large numbers of such objects even though we are confined to finding only the local ones (Tollerud et al. 2008). On the high surface brightness side, these objects become confused with stars (Hilker et al. 1999; Drinkwater et al. 2000; Phillipps et al. 2001) and therefore require unbiased redshift surveys to identify (for recent examples see Misgeld et al. 2011; Chiboucas et al. 2011). There are a handful of Galactic objects that might lie between the branches (Zaritsky et al. 2011) but these systems are all of low mass, highly susceptible to dynamical effects, and may therefore not satisfy the basic requirement of Eq. 1, which is that the system satisfy the virial theorem.

3.2. Theoretical Work

The physics of galaxy formation determines the relationship between Υ_h and the structural parameters of each galaxy. As such, we desire a theory that will explain the principle observables of each galaxy individually. Many attempts to reconcile the theory of galaxy formation as currently understood to observed scaling relations (either one for spheroids or disks) exist (for some examples see Dutton & van den Bosch 2012, and references therein). The key to these models is how one follows the complicated physics of galactic feedback and angular momentum transfer between the baryons and dark matter. The models can reproduce general galaxy properties if one artificially imposes how these effects scale with halo mass. Of course, the next question is why such recaling exists. Dutton & van den Bosch (2012) conclude that certain processes, such as the angular momentum evolution of galaxy disks, are not yet sufficiently well understood to be modeled sufficiently accurately to reproduce the scaling relations. Empirical scaling relations provide challenging benchmarks for the models. Extending the range of these scaling relations, for example down to ultrafaint galaxies, is invaluable because it places even stronger constraints on hypothesized physical mechanisms. For example, Anderson & Bregman (2010) and McGaugh (2012) used the baryonic TF relation to argue that there are basic conceptual problems with feedback models, while Dutton (2012) then used this argument to examine how to obtain plausible models for star formation and feedback. This article is not intended as review

of theoretical models, but such modeling is critically dependent on the best possible empirical constraints. Because current simulations lack the ability to treat the physical processes in detail and realistically, they are not reliably predictive and must constantly be compared to the available constraints.

4. APPLICATIONS OF THE FM

Although understanding galaxy formation remains the principal goal behind refining and understanding the FM, the relationship also has various uses that do not require a theoretical underpinning. For example, as with the FP and TF before it, the FM can be used as a distance estimator because r_h is in physical (distance dependent) units.

4.1. Using the Scaling Relationships for Distance Measurements

The advantages that the FM provides over its antecedents come from its universality. For example, the FM is applicable to low luminosity local systems, in which individual stars are resolved but neither the FP or TF apply. This capability is critical because certain distance methods require resolved stellar populations, which are beyond our current technology's reach for most of the galaxies that we know satisfy the FP and TF. As such, the FM can be used to cross-calibrate distance estimators even when those estimators are not found in the same galaxy. For example, Figure 4 (reproduced from Figure 2 of Zaritsky et al. (2011)) illustrates why it is difficult to compare distances obtained from surface brightness fluctuations (SBF) and Cepheids if one requires having distance estimates for the same galaxy from the two methods. Likewise, certain methods tend to work over limited distance ranges and are therefore not suitable for comparison with other. Using the FM as a fiducial, distances obtained using SN Ia, Cepheids, SBF, the luminosity of the tip of the red giant branch (TRGB), circumnuclear masers, eclipsing binaries, RR Lyrae stars, and the planetary nebulae luminosity functions (PNe) were compared by Zaritsky et al. (2011).

This comparison is done by placing galaxies with independent distance measures on the FM, using the distance from each particular distance estimator to convert r_h from angular to physical units. In Figure 5 we reproduce Figure 7 from Zaritsky et al. (2011) that presents the FM relationship derived using the distance measurements obtained from each type of distance estimator for which there are at least 10 galaxies with all the necessary data. The velocity dispersion dominated systems, which have measured velocity dispersions and sometimes also have stellar rotation values, are plotted in the upper panels of the Figure and the purely rotationally supported galaxies, which have no quoted stellar velocity dispersion and where the inclination-corrected H I width is adopted as a measure of v_r , are plotted in the lower panels. In general, if there is a stellar velocity dispersion measurement, the galaxy is a pressure supported systems ($v_r/\sigma_v < 1$). Within each panel a color-code describes morphology, dividing the early and late type galaxies at a T-Type of 1. The zero point of the FM is set using the results from the pressure-supported, SBF sample, which is the largest subsample of galaxies and also predominantly consists of early-type galaxies, which are

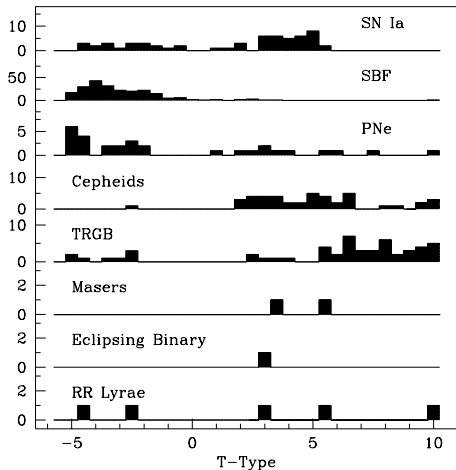


Figure 4. Distribution of morphological types as a function of distance measuring technique among a sample drawn from NED-1D. The Y-axis is arbitrarily normalized to match scales among subsamples. Differences among the types of galaxies accessible to various methods are clear (adopted directly from Figure 2 of Zaritsky et al. 2011)

less susceptible to extinction and stellar population variations. Although many more galaxies than those shown have distances measured using at least one of these methods, many of those lack the measurements necessary to place them on the FM. The solid lines represent the FM and the only “free” parameter involved here is the normalization applied to get the mean SBF relation exactly (on average) on the FM. Normalization or slope errors for any particular distance estimator suggests that there is a problem with that estimator. Increased scatter suggests a lower precision for that particular distance estimator.

A cursory examination of the panels reveals no serious problems with any of the distance estimators as applied to any of the galaxy subsamples, even though some perform better than others (either in terms of zero point or scatter). There are a few individual galaxy outliers, although it is often the same galaxy that is an outlier in multiple panels because distances are sometimes available from multiple estimators, suggesting that fault lies not with the distance estimate but rather with one of the other parameters that enters the FM. There are no statistically significant differences in zero point between the distance estimators (Zaritsky et al. 2011), although the allowed differences are still above the level of precision (\sim percent) that is the goal of current studies. Increasing the sample significantly, which is well within what can be done with a reasonable investment of resources, will provide stricter limits on potential systematic differences among estimators.

Zaritsky et al. (2011) also examined the FM residuals within a given distance estimator vs. other potential sources of systematic error. For example, they examined the relationship between FM residual and host galaxy metallicity for distances derived using SNe Ia, they found a correlation, confirming previous claims of metallicity-dependent correction to the Ia distances (Gallagher et al. 2008; Howell et al. 2009; Romaniello et al. 2008).

Once established as a distance estimator itself, the

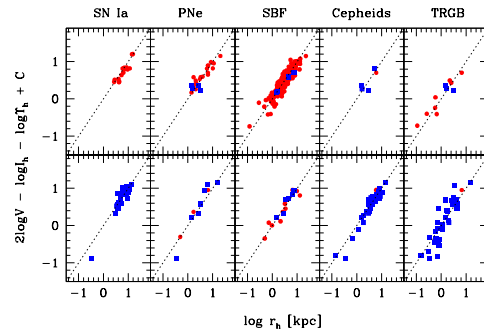


Figure 5. FM using measured distances. A comparison of the FM’s obtained using different distance estimators. The sample is divided into pressure supported (upper panels) and rotationally supported (lower panels). Furthermore, color and shape codes distinguish galaxy morphologies (blue squares for late type, red circles for early type). The x axis is $\log r_h$ in kpc, and the y-axis is $2 \log V - \log I_h - \log Y_h - C$, where V is in km sec^{-1} , I_h is in $L_\odot/\text{sq. pc}$, and Y_h is in solar units. C is obtained by calibrating to the sample of surface brightness fluctuation distances (SBF) for the pressure supported galaxies. The line is the 1:1 expectation, not a fit to the data (adopted directly from Figure 7 of Zaritsky et al. 2011).

FM can be used for a large set of galaxies. In Figure 6, I reproduce Figure 12 of Zaritsky et al. (2011) that shows the relationship between recessional velocity and distance obtained from the FM for the same set of galaxies shown in Figure 5. Comparing between different normalization of the distances, using the various distance estimators available to them, Zaritsky et al. (2011) cite a systematic uncertainty of $4 \text{ km sec}^{-1} \text{ Mpc}^{-1}$ in H_0 . The inset shows the result of fitting the relationship for galaxies with $v > 1500 \text{ km sec}^{-1}$, 3σ outliers excluded, binned by 10, with the fit forced through the origin. The low v region is excluded to minimize the effect of local flows. They find a best fit slope corresponding to $H_0 = 78 \pm 2$ (random) ± 4 (systematic) $\text{km sec}^{-1} \text{ Mpc}^{-1}$. The estimate of the systematic uncertainty does not include a variety of potential problems that they ignored (modeling of bulk flows, internal extinction corrections, adjustment for potential biases in the galaxy sample, etc.), but this calculation was done primarily as a plausibility exercise to demonstrate the use of the FM.

One of those sources of uncertainty, internal extinction, would be mitigated by going to the infrared, as shown most recently by Freedman & Madore (2011) for *Spitzer* wavelengths where the scatter about the TF relation is reduced from 0.43 in the extinction-corrected B -band data to 0.31 in the non-extinction-corrected $3.6\mu\text{m}$ data. One avenue for advancement is therefore the use of large IR photometric galaxy samples (Sheth et al. 2010).

The most straightforward way for advancement is to obtain kinematic measurements for a large number of galaxies with existing distance measurements. In Figure 7 I present a subset of galaxies with SNe Ia distance measurements and highlight those for which all the necessary data are available. An interesting indication of how these data may help refine distances is provided by two outliers from the FM (at 50 Mpc and the one da-

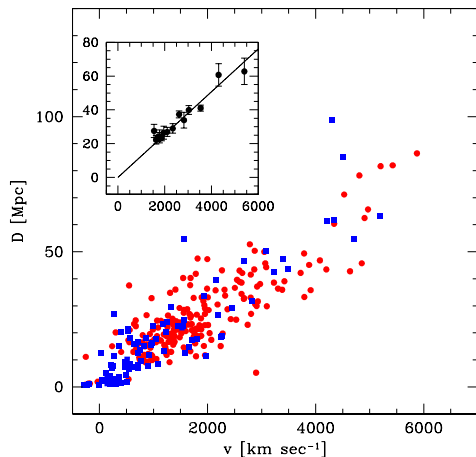


Figure 6. Hubble diagram using distances derived using the FM. Pressure supported systems are plotted as red circles and rotationally supported systems as blue squares. Inset shows data at $v > 1500$ km sec $^{-1}$ binned so that each bin contains 10 galaxies. The fitted line is constrained to go through the origin and corresponds to $H_0 = 78 \pm 2$ (random) ± 4 (systematic) km sec $^{-1}$ Mpc $^{-1}$ (adopted directly from Figure 12 of Zaritsky et al. 2011)

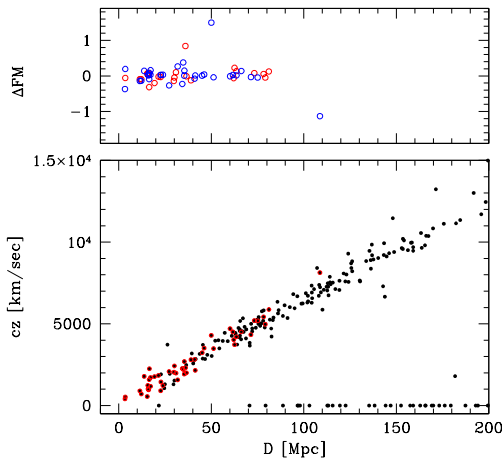


Figure 7. SN Ia distances and the FM. The upper panel shows the residuals about the FM relation (ΔFM) for galaxies with SN Ia distances. Blue and red symbols denote rotationally and pressure supported systems respectively. The bottom panel shows the Hubble diagram for galaxies with SN Ia distances available in the NED 1-D database. The galaxies with all the necessary data to be placed on the FM are highlighted in red. There are numerous galaxies with existing SN Ia distances that could be added to the FM with reasonable observational effort. The most noticeable outliers from the FM are also outliers in the Hubble diagram.

tum beyond 100 Mpc), which are both outliers in the SNe Hubble diagram. That these galaxies are outliers in both panels suggests that there is a problem with the distance. With larger samples, one could then attempt to find the cause for the distance anomaly by comparing with other characteristics, either those of the SNe itself or those of the host galaxy. Refining the SNe distances has broad implications for cosmology.

4.2. Using the Scaling Relationships for Mass Measurements

The stellar mass of a galaxy is intricately connected to a variety of galaxy properties: environment (Kauffmann et al. 2004), metal abundance (Tremonti et al. 2004), star formation history (Bundy et al. 2006), and dark matter halo mass (van den Bosch et al. 2003), to name a few. However, the stellar mass estimates we rely on are quite crude and potentially rife with systematic errors. A seemingly straightforward way to estimate the stellar mass is to use measurements of the stellar populations, such as color, to estimate Υ_* and to convert the luminosity into a mass. However those estimates depend on three factors that are not well understood: 1) the galaxy’s star formation history, which can be quite complex (see for examples Harris & Zaritsky 2004, 2009; Eskew & Zaritsky 2011; Weisz et al. 2011) 2) stars’ behavior during the phase(s) of their life at which they are at their most luminous, which is problematic (Maraston et al. 2006; Conroy, Gunn, & White 2008; McQuinn, et al. 2011; Melbourne et al. 2012) and 3) the initial distribution of stellar masses (the initial mass function or IMF), which is a well-known unresolved problem (Bastian et al. 2010). An alternative method is to dynamically measure the mass and, if necessary, make a correction for the amount of dark matter present. The FM enables us to measure the total masses within r_h .

An interesting set of stellar systems to examine are stellar clusters, which presumably contain no dark matter and are single age populations. As such, the estimates of Υ_h obtained using the FM provide a measurement of the mass-to-light ratio of a stellar population, Υ_* , of a certain age. A large compilation of Local Group stellar cluster data was published by McLaughlin & van der Marel (2005), although the velocity dispersions available at the time of that study were either for the older (> 10 Gyr) clusters or the very young ones (< 100 million yr). Zaritsky et al. (2012) filled in this range by observing clusters over the full range of ages.

Discrepancies between models and observations of galaxies, when found, are often attributed to deviations in the IMF from the adopted prescription (for some recent examples see van Dokkum 2008; Dabringhausen et al. 2009; Treu et al. 2010; van Dokkum & Conroy 2010; Dutton et al. 2012) rather than problems with either the star formation history or stellar evolutionary models. However, direct measurements of the initial mass function are difficult for various reasons (see Bastian et al. 2010, for a review), particularly over the full range of environments and conditions. These clusters provide one of the most direct tests of the IMF.

The principal empirical result presented by Zaritsky et al. (2012), the relationship between Υ_* and age, is reproduced in Figure 8 (their Figure 9 reproduced here). The naive expectation, that Υ_* rises continually with age is evidently not reproduced by the data. Internal dynamics, principally two-body relaxation which causes preferential loss of low mass stars over time (Spitzer 1958; Kruijssen 2008), plays a role here, but it is insufficient to explain the large

drop in Υ_* between a few and 10 Gyr. Zaritsky et al. (2012) support this claim by applying the dynamical models of Anders et al. (2009). A second possible reason for why the naive expectation may not be met is the influence of binary stars, which can artificially inflate the observed velocity dispersion of a system (for examples see Minor et al 2010; Gieles et al. 2010). Again the effects are considered and found to be too weak to explain the observations or too contrived, requiring unknown an binary population that affects the kinematics of ~ 1 Gyr populations but not those of age $>$ few Gyr. Variations in the initial mass function among these systems is a viable explanation.

In the same Figure, Zaritsky et al. (2012) also included two model tracks for the evolution of simple stellar populations. First, the plotted values of Υ_* for the stellar clusters are corrected for the effect of internal dynamical evolution using the results of the Anders et al. (2009) models. They plot the results of PEGASE models (Fioc & Rocca-Volmerange 1997) using a Salpeter (1955) IMF, spanning from 0.1 to 120 M_\odot , with default stellar mass loss and binarity parameters, and metallicity matching the mean of the young clusters (-0.4). These model values are not renormalized in any way and yet do an acceptable job of reproducing the trend seen in the younger clusters, for clusters of $8 < \log(\text{age} [\text{yrs}]) < 9.4$. Discrepancies at younger ages can be ignored due to the likelihood that these clusters are not relaxed (Goodwin & Bastian 2006). The second model is that of a lightweighted Kroupa (2001) IMF, where $\sim 50\%$ of the mass is removed (lightweighted) to produce the match in the Figure. A Charbrier (2003) IMF works similarly. One interpretation of this Figure hypothesizes the presence of two IMFs for star clusters, one IMF being primarily, but not exclusively, appropriate for older, metal poor clusters and the other for primarily, but not exclusively, for younger, metal rich clusters. The young ($\log(\text{age} [\text{yrs}]) < 9.5$) clusters are well-described by a bottom-heavy IMF, such as a Salpeter IMF, while the older clusters are better described by a top-heavy IMF, such as a lightweighted Kroupa IMF, although neither of these specific forms is a unique solution. Ongoing work will at least double the sample size, but we will eventually need to obtain high resolution deep imaging of the intermediate age clusters to confirm that these have a bottom heavy mass function. While some work has been done with *HST* (Glatt et al. 2011), deeper, less ambiguous results are necessary to definitively prove or disprove this interpretation. Such work is within reach of adaptive optics on large telescopes.

In addition to stellar clusters, the FM can also be applied to estimate the masses (within r_h) of galaxies across cosmic time. In particular, this approach can test the hypothesis that large deviations from stellar evolutionary models, rather than IMF variations, are responsible for sudden drop in Υ_* after a few Gyr. Using measurements of the ages and structural parameters of two independent sets of early type galaxies, Zaritsky et al. (2012) compared the derived values of Υ_h to those derived for the clusters. Such comparisons constrain both Υ_* and the fraction of the mass in the form of dark matter within r_h . They used both a study of Sloan Digital Sky Survey (SDSS) local galaxies presented by Graves et al. (2009) and a study of galaxy cluster FP measurements

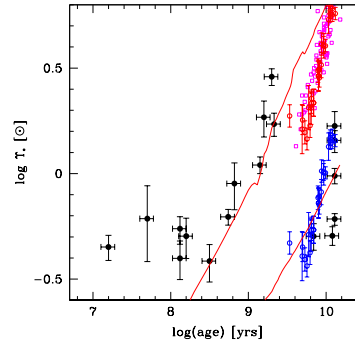


Figure 8. The evolution of Υ_* as inferred from early type galaxies and comparison to models and our cluster data. The stellar cluster data are plotted in solid circles (black), the results obtained using the results from van Dokkum & van der Marel (2007) are plotted with open circles (red) when normalized to match the results from the sample of Graves et al. (2009), which are plotted with squares (pink). Also shown are the van Dokkum & van der Marel (2007) data assuming a dark matter fraction of 80%, so as to qualitatively match to the stellar cluster data, in open circles (blue). The dark matter fraction is likely to be somewhere between 0 and 80%. The upper solid line represents the values of Υ_h from a PEGASE model of a population with an instantaneous burst at $t = 0$ and a Salpeter IMF, while the lower represents a model with a light-weighted Kroupa IMF (adopted directly from Figure 9 of Zaritsky et al. (2012)).

presented by van Dokkum & van der Marel (2007). The latter study provides only differences in Υ_h as a function of redshift, so global shifts of Υ_h are allowed. The results of those studies are include in Figure 8 for comparison to the cluster values (after the van Dokkum & van der Marel (2007) data were normalized to match the Graves et al. (2009) data). An important distinction for the galaxy results, is that these systems do contain dark matter and that the exact proportion of dark matter within r_h is unknown and likely to vary as a function of the structural parameters (for some examples from the long history of this topic see Babul & Rees 1992; Graham 2002; Marinoni & Hudson 2002; van den Bosch et al. 2003; Cappellari et al. 2006; Zaritsky et al. 2006a; Wolf et al. 2010).

The comparisons between clusters, galaxies and models provide several interesting results. The early-type galaxies lie between the extrapolation of the young cluster trend and that of the old clusters. Because of the dark matter content of galaxies, the actual value of Υ_* for the galaxies is likely to be lower than that plotted. This suggests that they will not lie on the track defined by the young clusters, which is already slightly above the galaxy data⁶. On the other hand, unless the dark matter fraction is quite large ($\sim 80\%$, the blue points in the Figure), the ellipticals will not resemble the old clusters either. Although the possibility of such a large DM fraction is not excluded, we may be seeing the effects of having a mixture of populations of stars, some with the IMF of the old clusters and some with that of the young clusters. However, there is no strong deviation from the general behavior predicted by simple stellar evolutionary models and so that does not appear to be the cause of

⁶ Careful modeling is necessary to reach robust conclusions because the galaxies are not necessarily single age populations. If an old galaxy has a small population of younger stars, those stars will lower the effective Υ of the galaxy.

the behavior of Υ_* in the stellar cluster sample.

5. SUMMARY

Order implies rules. Rules governing the structure of dynamical systems are the manifestation of underlying physics. Understanding this physics is the overarching goal of the study of galaxy formation and evolution. Is there order among galaxies?

In the early days of modern astronomy, the morphological appearance of galaxies was the principal characteristic that dominated attempts at describing order among galaxies (Hubble 1926; Sandage 1961). This approach has been mostly upended by 1) the realization that accretion and mergers drive galaxy evolution and alter morphologies, 2) the dynamical importance of dark matter, which clearly is not a part of a morphological scheme, 3) the increasingly quantitative nature of astronomy and large digital surveys, and 4) the discovery of scaling relations such as the Fundamental Plane (FP) and Tully-Fisher (TF). In this review, I have described the development of a scaling relation that is an extended version of the FP, called the Fundamental Manifold (FM), that works on all classes of stellar systems and exhibits a scatter comparable to the more restrictive FP and TF relations.

The FM relationship depends on three distinct conditions being satisfied: 1) that the virial theorem is applicable, 2) that the derived mass enclosed within the half-light radius, r_h , be at most only weakly dependent on the distribution function of the tracer particles and the gravitational potential, and 3) that the mass-to-light ratio within r_h , Υ_h , depend on at most the observed parameters V_h and I_h . The first is as expected because we are working with systems that are virialized ($r_h \ll r_{200}$). The second is somewhat surprising, but has now been verified at least for spheroidal systems, which are the ones that are most likely to have large variations among distribution functions, by the work of Walker et al. (2009) and Wolf et al. (2010). The last still requires explanation, although it is manifestly a critical component of a complete theory of galaxy formation and evolution.

Going forward there are several areas that will yield immediate returns. First, homogenous samples across galaxy type with detailed kinematics so that there is uniform, high quality data across the parameter space are critical to testing Equation 7, measuring the parameter that relates velocity dispersion and rotation, α , and determining the intrinsic scatter about the relation as a function of galaxy mass and morphology. Second, an improved understanding of the initial mass function is key to accurate and precise calculations of Υ_* . Determining Υ_* is necessary to uncovering the behavior of dark matter as a function of mass and galaxy type. Third, direct application of the FM to a number of topics, including distance determinations, will yield results even if a deeper understanding of galaxy formation remains elusive in the short term. The FM, like the FP and TF before it, should help propel research forward in a wide range of topic areas.

The author acknowledges the close collaboration with Ann Zabludoff and Anthony Gonzalez during which most

of the material reviewed here was developed. The author acknowledges financial support for this work from a NASA LTSA award NNG05GE82G and NSF grant AST-0307482 as well as the hospitality of NYU CCPP during his many visits.

REFERENCES

- Aaronson, M., & Mould, J. 1983, *ApJ*, 265, 1
 Anders, P., Lamers, H.J.G.L.M., & Baumgardt, H. 2009, *A&A*, 502, 817
 Anderson, M.E., & Bregman, J.N., 2010, *ApJ*, 714, 320
 Babul, A., & Rees, M.J. 1992, *MNRAS*, 255, 346
 Bahcall, J. N., & Tremaine, S. 1981, *ApJ*, 244, 805
 Bastian, N., Covey, K.R., & Meyer, M.R. 2010, *Ann. Rev. Astron. Astroph.*, 48, 339
 Bedregal, A.G., Aragón-Salamanca, A., & Merrifield, M.R. 2006, *MNRAS*373, 1 125
 Bender, R. 1990, *A&A*, 229, 441
 Bernardi, M. et al. 2003, *AJ*, 125, 1866
 Bernardi, M., Roche, N, Shankar, F., & Sheth, R.K. 2011, *MNRAS*, 412, 6
 Bolton, A. S., Treu, T., Koopmans, L. V. E., Gavazzi, R., Moustakas, L. A., Burles, S., Schlegel, D. J. & Wayth, R., 2008, *ApJ*, 683, 248
 Bundy, K. et al. 2006, *ApJ*, 651, 120
 Burstein, D. & Bender, R. & Faber, S. & Nolthenius, R., 1997, *AJ*, 114, 1365
 Cappellari, M. et al. 2006, *MNRAS*, 366,1126
 Cappellari, M. et al. 2012, submitted to *MNRAS*, arXiv:1208.3523
 Chabrier, G., 2003, *PASP*, 115, 763
 Chiboucas, K. et. al. 2011, *ApJ*, 737, 86
 Conroy, C., Gunn, J. E. & White, M., 2008,
 Courteau, S., Dutton, A.A., van den Bosch, F.C., MacArthur, L.A., Dekel, A., McIntosh, D.H., & Dale, D.A. 2007, *ApJ*, 671, 203
 Cretton, N., de Zeeuw, P.T., van der Marel, R.P., & Rix, H.W.R. 1999, *ApJ*, 124, 383
 Dabringhausen, J., Kroupa, P., Baumgardt, H. 2009, *MNRAS*, 394, 1529
 Dalcanton, J.J., Spergel, D.N., & Summers, F.J. 1997, *ApJ*, 482, 659
 Davies, R. L., Efstathiou, G., Fall, S.M., Illingworth, G., Schechter, P.L. 1983, *ApJ*, 266, 41
 Dejonghe, H. 1987, *MNRAS*, 133, 217
 Djorgovski, S. & Davis, M., 1987, *ApJ*, 313, 59
 Dressler, A. & Lynden-Bell, D. & Burstein, D. & Davies, R. L., Faber, S. M., Terlevich, R. & Wegner, G., 1987, *ApJ*, 313, 42
 Drinkwater, M.J., Jones, J.B., Gregg, M.D., & Phillipps, S. 2000, *PASA*, 17, 227
 Dutton, A.A., 2012, *MNRAS* in press (arXiv:1206:1855)
 Dutton, A.A., Mendel, J.T., & Simard, L. 2010, *MNRAS*, 422, 33
 Dutton, A.A. & van den Bosch, F.C. 2012, *MNRAS*, 421, 608
 Erickson, K., Gottesman, S.T., & Hunter, J.H. Jr., 1987, *Nature*, 325, 779
 Eskew, M. & Zaritsky, D. 2011, *AJ*, 141, 69
 Eskew, M., Zaritsky, D., & Meidt, S. 2012, *AJ*, 143, 139
 Faber, S.M. & Jackson, R.E. 1976, *ApJ*, 204, 668
 Fall, S. M., & Efstathiou, G. 1980 *MNRAS*, 193, 189
 Fioc, M., & Rocca-Volmerange, B. 1997, *A&A*, 326, 950
 Forbes, D. A., Lasky, P., Graham, A. W., & Spitler, L., 2008, *MNRAS*, 389, 1924
 Freedman, W.L., & Madore, B.F., 2011, *ApJ*, 734, 46
 Gallagher, J. S., Garnavich, P. M., Caldwell, N., Kirshner, R. P., Jha, S. W., Li, W., Ganeshalingam, M. and Filippenko, A. V., 2008, *ApJ*, 685, 752
 Giesels, M., Sana, H., & Pertegies Zwart, S.F. 2010, *MNRAS*, 402, 1750
 Glatt, K. et al. 2011, *AJ*, 142, 36
 Goodwin, S. P., & Bastian, N. 2006, *MNRAS*, 373, 752
 Graves, G.J., Faber, S.M., & Schiavon, R.P. 2009, *ApJ*, 698, 1590
 Graham, A. 2002, *MNRAS*, 334, 721
 Harris, J., & Zaritsky, D. 2004, *AJ*, 127, 1531
 Harris, J., & Zaritsky, D. 2009, *AJ*, 138, 1243
 Heisler, J., Tremaine, S., & Bahcall, J.N. 1985, *ApJ*, 298, 8

- Hilker, M., Infante, L., Vieira, G., Kissler-Patig, M., & Richtler, T. 1999, *A&AS*, 134, 75
- Hoekstra, H., Hsieh, B.C., Yee, H.K.C., Lin, H., & Gladders, M.D. 2005, *ApJ*, 635, 73
- Howell, D.A. et al. 2009, *ApJ*, 691, 661
- Hubble, E.P. 1926, *ApJ*, 64, 32
- Jørgensen, I., Franx, M., & Kjaergaard, P. 1996, *MNRAS*, 280, 167
- Kassin, S.A., et al. 2007, 660, 35
- Kaufmann, G., White, S. D. M., Heckman, T., Ménard, B., Brinchmann, J., Charlot, S., Tremonti, C., & Brinkmann, J. 2004, *MNRAS*, 353, 713
- Khosroshahi, H.G., Wadadekar, Y., Kembhavi, A. & Mobasher, B. 2000, *ApJ*, 531, 103
- Kormendy, J. 1985, *ApJ*, 295, 73
- Kroupa, P. 2001, *MNRAS*, 322, 231
- Kruijssen, J.M.D. 2008, *A&A*, 486, 21
- Little, B., & Tremaine, S. *ApJ*, 320, 493
- Mandelbaum, R., Seljak, U., Kauffmann, G., Hirata, C., & Brinkmann, J. 2006, *MNRAS*, 368, 715
- Maraston, C., Daddi, E., Renzini, A., Cimatti, A. & Dickinson, M., Papovich, C., Pasquali, A., & Pirzkal, N., 2006, *ApJ*, 652, 85
- Marinoni, C., & Hudson, M.J. 2002, *ApJ*, 569, 101
- McGaugh, S.S. 2012 *AJ*, 143, 40
- McLaughlin, D. E. & van der Marel, R. P., 2005, *ApJS*, 161, 304
- McQuinn, K.B.W., Skillman, E.D., Dalcanton, J.J., Dolphin, A.E., Holtzman, J., Weisz, D., & Williams, B.F. 2011, *AJ*, 740, 48
- Meidt, S. et al. 2012, *ApJ*, 744, 17
- Melbourne, J., et al. 2012, *ApJ*, 748, 47
- Merrifield, M.,R. & Kent, S.M. 1990, *ApJ*, 99, 1548
- Mieske, S. et al. 2008, *A&A*, 487, 921
- Minor, Q.E., Martinez, G., Bullock, J., Kaplinghat, M., & Trainor, R. 2010, *ApJ*, 721, 1142
- Misgeld, I. & Hilker, M. 2011, *MNRAS*, 414, 3699
- Misgeld, I., Mieske, S., Hilker, M., Richtler, T., Gerogiev, I.Y. & Schuberth, Y. 2011, *A&A*, 531, 4
- Mould, J., Mingsheng, H., & Bothun, G. 1989, *ApJ*, 347, 112
- Page, T. 1952, *ApJ*, 116, 63
- Pasquato, M. & Bertin, G. 2008, *â*, 489, 1079
- Persic, M., & Salucci, P. 1991, *MNRAS*, 248, 325
- Phillipps, S., Drinkwater, M.J., Gregg, M.D., & Jones, J.B. 2001, *ApJ*, 560, 201
- Pizagno, J., et al. 2007, *AJ*, 134, 945
- Romaniello, M. et al. 2008, *A&A*, 488, 731
- Saintonge, A., & Spekkens, K. 2011, *ApJ*, 726, 77
- Salpeter, E.E. 1955, *ApJ*, 121, 161
- Salucci, P., Lapi, A., Tonini, C., Gentile, G., Yegorova, I., & Klein, U. 2007, *MNRAS*, 378, 41
- Salucci, P., Wilkinson, M.I., Walker, M.G., Gilmore, G.F., Grebel, E.K., Koch, A., Frigerio Martins, C., & Wyse, R. F. G. 2012, *MNRAS*, 420, 2034
- Sandage, A. 1961, *The Hubble Atlas of Galaxies*, (Washington: Carnegie Institution)
- Sheth, K., et al. 2010, *PASP*, 122, 1397
- Smith, M.A. & Gray, D.F. 1976, *PASP*, 88, 809
- Spitzer, L. 1958, *ApJ*, 127, 17
- Springel, V. et al. 2005 *Nature*, 435, 629
- Statler, T.S. 1987, *ApJ*, 321, 113
- Tollerud, E.J., Boylan-Kolchin, M., Barton, E.J., Bullock, J.S., & Trihn, C.Q. 2011, *ApJ*, 738, 102
- Tollerud, E.J., Bullock, J.S., Strigari, L. E., & Willman, B. 2008, *ApJ*, 688, 277
- Tremonti, C.A. et al. 2004, *ApJ*, 613, 898
- Treu, T., Auger, M.W., Koopmans, L.V.E., Gavazzi, R., Marshall, P.J., & Bolton, A.S. 2010, *ApJ*, 709, 1195
- Tully, R. B. and Fisher, J. R., 1977, *A&A*, 54, 661
- van den Bosch, F. C., Yang, X., Mo, H.J. 2003, *MNRAS*, 340,771
- van der Marel, R.P., & van Dokkum, P.G. 2007, *ApJ*, 668, 756
- Vandervroot, P. O. 1984, *ApJ*, 287, 475
- van Dokkum, P.G., 2008, *ApJ*, 674, 29
- van Dokkum, P.G., & Conroy, C. 2010, *Nature*, 468, 940
- van Dokkum, P. G., & van der Marel, R. P. 2007, *ApJ*, 655, 30
- Walker, M.G., Mateo, M., Olszewski, E.W., Peñarrubia, J., Wyn Evans, N., & Gilmore, G. *ApJ*, 704, 1274
- Weiner, B. et al. 2006, *ApJ*, 653, 1049
- Weisz, D., et al. 2011, *ApJ*, 739, 5
- Willman, B. & Strader, J. 2012, *AJ*, in press
- Wolf, J., Martinez, G.D., Bullock, J.S., Kaplinghat, M., Geha, M., Muñoz, R.R., Simon, J.D., & Avedo, F.F. *MNRAS*, 406, 1220
- Yang, X., Mo, H.J., Jing, Y.P., & van den Bosch, F.C. 2005, *MNRAS*, 358, 217
- Yegorova, I.A. & Salucci, P. 2007, *MNRAS*, 377, 507
- Zaritsky, D., Colucci, J., Pessev, P., Bernstein, R.A., & Chandar, R. 2012, *ApJ*, in press
- Zaritsky, D., Gonzalez, A. H. & Zabludoff, A. I., 2006a, *ApJ*, 638, 725
- Zaritsky, D., Gonzalez, A. H. & Zabludoff, A. I., 2006b, *ApJ*, 642, L37
- Zaritsky, D. & White, S.D.M. 1994, *ApJ*, 435, 599
- Zaritsky, D., Zabludoff, A. I. & Gonzalez, A. H., 2008, *ApJ*, 682, 68
- Zaritsky, D., Zabludoff, A. I. & Gonzalez, A. H., 2011, *ApJ*, 727, 116
- Zaritsky, D., Zabludoff, A. I. & Gonzalez, A. H., 2012, *ApJ*, 758, 15
- Zhu, G., Blanton, M.R., & Moustakas, J. 2010, *ApJ*, 722, 491